JEMAT 2025, Vol 13, No 2, 45-56
https://doi.org/10.54987/jemat.v13i2.1172

JOURNAL OF ENVIRONMENTAL MICROBIOLOGY AND TOXICOLOGY

Website: http://journal.hibiscuspublisher.com/index.php/JEMAT/index

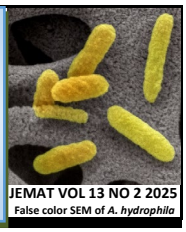

Response Surface Optimization of Acetylcholinesterase Extraction from *Scomberomorus commerson* for Toxicological Applications

Darren Guo Bin Beh[1] and Mohd Yunus Shukor[1]*

[1]Department of Biochemistry, Faculty of Biotechnology and Biomolecular Sciences, Universiti Putra Malaysia, 43400 UPM Serdang, Malaysia.

*Corresponding author:
Mohd Yunus Shukor,
Department of Biochemistry,
Faculty of Biotechnology and Biomolecular Sciences,
Universiti Putra Malaysia,
43400 UPM Serdang,
Malaysia.
Email: mohdyunus@upm.edu.my

History

Received: 29th Oct 2025
Received in revised form: 19th Dec 2025
Accepted: 12th Dec 2025

Keywords

Acetylcholinesterase (AChE)
Extraction optimization
Response Surface Methodology (RSM)
Box-Behnken Design (BBD)
Toxicology biomonitoring

SDG Keywords

SDG 3 – Good Health and Well-Being
SDG 12 – Responsible Consumption and Production
SDG 14 – Life Below Water

Abstract

Cholinesterase, especially acetylcholinesterase, is often used in toxicology research in insecticide biomonitoring work from the environment or from agricultural products. One of the most utilized sources of acetylcholinesterase is from fish acetylcholinesterase, and the search for potentially sensitive sources of acetylcholinesterase is ongoing research. In this study, the extraction conditions of acetylcholinesterase (AChE) from *Scomberomorus commerson,* a novel source, were optimized using Response Surface Methodology (RSM). A Box-Behnken Design (BBD) was applied to evaluate the effects of three independent variables—pH (7.0-8.8), NaCl concentration (0.05-0.20 M), and Triton X-100 concentration (0.01-0.04% v/v)—on AChE activity as the response. Experimental data were fitted to a quadratic polynomial model, which demonstrated good agreement with the observed values ($R^2 = 0.9081$; Adj $R^2 = 0.7898$). Analysis of variance confirmed that pH was the most significant factor influencing extraction efficiency ($p < 0.01$), while NaCl and Triton X-100 showed weaker individual effects within the studied range. A significant interaction between pH and NaCl ($p < 0.05$), together with the quadratic effect of pH, contributed to the nonlinear extraction profile. Numerical optimization predicted maximum AChE activity at pH 8.79, 0.197 M NaCl, and 0.039% Triton X-100, yielding a predicted activity of 0.145 U (95% CI: 0.125-0.166 U). Experimental validation produced a similar value of 0.152 U, confirming the reliability of the model. Further kinetic characterization revealed substrate-dependent variations in catalytic parameters, with V_{max} and K_m values of 0.02238 U and 0.03387 mM for acetylthiocholine (ATC), 0.02135 U and 0.2177 mM for propionylthiocholine (PTC), and 0.01928 U and 0.2316 mM for butyrylthiocholine (BTC), respectively. These findings demonstrate that RSM is an effective approach for improving AChE extraction, with pH identified as the primary factor governing extraction performance.

INTRODUCTION

Acetylcholinesterase (AChE; EC 3.1.1.7) is an enzyme present in the synaptic cleft. It has the role to break down the acetylcholine (ACh), which is a neurotransmitter, into acetic acid and choline. This prevents the transmission of signals between neurons. In the brain, especially the hippocampus and cortex, ACh is involved in high-order thinking such as learning, memorizing, and attention. AChE controls the concentration of the ACh in the synapses, which improper function will disrupt the balance of ACh, which causes overstimulation of the receptors or poor synaptic transmission. Alzheimer's disease is a progressive neurodegenerative disorder. Currently, 51.6 million individuals globally are affected [1]. It has become a major health concern, especially for people aged 65 and above. It is predicted that 152.8 million individuals will be affected by Alzheimer's Disease by 2050 [2]. Despite advancements in early detection, effective treatment remains limited. AChE inhibitors are one of the few approved therapeutic options used to control the symptoms of Alzheimer's Disease. Therefore, AChE remains a crucial target in the development of drugs aimed to treat Alzheimer's disease [3].

AChE is also widely used as a biomarker for detecting exposure to toxic substances, such as organophosphate pesticides, which inhibit AChE activity and lead to harmful physiological effects [4]. Organophosphates and carbamates are widely used in agriculture as pesticides. However, due to its widespread application, its toxicity to public health has become a global concern. An analysis of pesticide poisoning from 2006

to 2015 revealed a rising trend, with an estimated average incidence rate of 3.8 per 100,000 individuals [5]. Given its diverse applications, the extraction of AChE is important to ensure accurate research outcomes. Efficient extraction of the enzyme is essential for obtaining reliable results in drug screening, toxicity testing, and biosensor development. However, traditional methods of optimization for enzyme extraction can be time-consuming, costly, and require a large number of experiments. To address these challenges, Response Surface Methodology (RSM**)** is increasingly used as a powerful statistical tool to optimize complex processes. RSM allows researchers to evaluate the effects of multiple variables and their interactions simultaneously while minimizing the number of experimental trials [6]. It also provides visual interpretations of data through surface and contour plots, making it easier to identify optimal conditions. In the context of enzyme extraction, RSM offers a practical and efficient approach to enhance yield and activity while reducing experimental effort.

Most studies focus on acetylcholinesterase activity or inhibition, rather than the step-by-step optimization of the extraction conditions. Few papers provide detailed descriptions of the extraction process aimed at maximizing both the activity and yield of the enzyme from specific biological sources, such as brain tissue. Additionally, the application of Response Surface Methodology (RSM) in acetylcholinesterase extraction is limited. RSM is used in optimizing acetylcholinesterase extraction from *Clarias batrachus*'s brain by Nazri et al. [7] and it effectively increased the yield and activity of AChE. This methodology holds significant promise for improving the cost-efficiency and overall extraction process of acetylcholinesterase.

Acetylcholinesterase (AChE) is an enzyme that plays a vital role in neurological function and is widely used in biomedical research, drug development, and environmental toxicity studies. However, the extraction of AChE from biological sources such as *Scomberomorus commerson* remains difficult due to factors such as complex tissue matrix, enzyme instability, and variability in extraction parameters. These lead to low enzyme recovery, reduced activity and inconsistent extract quality, which limit the reliability for downstream applications. There are a lack of studies focusing on systematic optimization of AChE extraction from *Scomberomorus commerson*, particularly, the use of RSM to determine the optimal conditions for AChE extraction.

Although *S. commerson* is well documented in these research areas, studies focusing specifically on AChE extraction from this species remain limited, no studies to date have reported the use of RSM for optimizing AChE extraction from *S. commerson*. Unlike prior RSM optimization in catfish (Clarias batrachus), this study applies a marine-derived AChE source with distinctive ionic requirements. The aim of this study is to optimize the AChE extraction from the brain of *Scomberomorus commerson* using RSM.

MATERIALS AND METHODS

Sample Preparation

Fresh heads of *Scomberomorus commerson* were purchased from the local wet market in March 2025 and transported to the laboratory in an ice-cooled container to minimize enzymatic degradation. Upon arrival, the fish's heads were rinsed with cold distilled water to remove surface contaminants. The head was carefully dissected to collect the brain tissue. The brain tissue was collected in a beaker surrounded by ice and weighed before it was homogenized.

Optimization of Extraction using OFAT

Firstly, the acetylcholinesterase (AChE) extraction conditions were optimized using one-factor-at-a-time (OFAT) method, in which only one extraction parameter was changed at a time. Three extraction parameters were optimized, which are the pH of the buffer, the Triton X-100 concentration and the NaCl concentration. The brain tissue was homogenized in a precooled deionized water at a ratio of 1g of brain to 4 mL of deionized water. Homogenization was carried out for 1 minute, with intermittent homogenization at 10-second intervals to reduce heat generation. Next, the homogenate was added into microcentrifuge tubes that contained the extraction buffer with pH value range from 5.8 to 8.8. Then the mixture was mixed using a vortex for 20 seconds. After mixing, the mixture was centrifuged at 10,000×g for 10 minutes [8]. Lastly, the supernatant was collected and subjected to AChE activity measurement. These steps were repeated to optimize the NaCl concentration and Triton X-100 concentration.

Optimization of Extraction using RSM

Response surface methodology (RSM) was used to optimize the AChE extraction condition following the initial screening using OFAT approach. The experimental design, statistical analysis, model fitting, and response surface plotting were performed using Design-Expert® software. Three extraction parameters were optimized as in OFAT, which are the pH of the buffer, the Triton X-100 concentration, and the NaCl concentration. The combined effect of these parameters on AChE activity was examined using a Box-Behnken design (BBD).

Table 1. Coded and uncoded levels of the independent variables used in the Box-Behnken design.

Parameter	Type	Sub Type	Min	Max	Coded Low	Coded High	Mean	SD
pH	Numeric	Continuous	7	8.8	-1↔7	+1↔8.8	7.9	0.6364
NaCl (M)	Numeric	Continuous	0.05	0.2	-1↔0.05	+1↔0.2	0.125	0.0530
Triton X-100 (%)	Numeric	Continuous	0.01	0.04	-1↔0.01	+1↔0.04	0.025	0.0106

Note* Min - Minimum. Max - Maximum. SD - Standard deviation.

The code and uncoded level of the extraction parameter used in BBD are summarized in **Table 1**. A three-factor experimental design consisting of 17 experimental runs was performed. The center point was included, which allows detection of experimental error and assessment of model effectiveness. The experimental design matrix and factor level combination for each run are shown in **Table 2**.

Table 2. Experimental design matrix for RSM optimization of acetylcholinesterase (AChE) extraction condition.

Run	Extraction Parameter		
	pH	NaCl concentration (M)	Triton X-100 concentration (%)
1	7.0	0.125	0.04
2	7.9	0.125	0.025
3	7.9	0.125	0.025
4	7.9	0.2	0.01
5	7.9	0.05	0.01
6	7.9	0.05	0.04
7	7.9	0.2	0.04
8	7.9	0.125	0.025
9	7	0.2	0.025
10	8.8	0.05	0.025
11	8.8	0.125	0.01
12	7	0.125	0.01
13	7.9	0.125	0.025
14	8.8	0.125	0.04
15	8.8	0.2	0.025
16	7.9	0.125	0.025
17	7	0.05	0.025

The brain was homogenized under the specific condition based on **Table 1** and centrifuged to obtain the supernatant. The supernatant was collected and subjected to AChE activity measurement. A second-order polynomial (quadratic) model was fitted to the experiment data. It determined the relationship between the extraction parameter and the AChE activity. The equation is as follows:

$$y = \beta_0 + \sum_{i=1}^{k} \beta_i x_i + \sum_{i=1}^{k} \beta_{ii} x_{ii}^2 + \sum_{i=1}^{k-1} \sum_{j>1}^{k} \beta_{ij} x_i x_j + \text{error} \quad \text{(Eqn. 2)}$$

where y is the estimated response variable, β_0 is the regression constant, β_i is the linear regression coefficient, β_{ii} is the quadratic regression coefficient, β_{ij} is the bi-linear regression coefficient. The quality of the model was evaluated using analysis of variance (ANOVA), coefficient of determination (R^2), adjusted R^2, Predicted R^2, lack-of-fit testing and adequate precision as described by Mororó et al. [24]. The response surface 3D plots were generated to visualize the effects and the interaction of the extraction parameters on AChE activity.

Model Validation

Next, Model Validation was conducted to verify the reliability and the predictive accuracy of the RSM model. The optimal extraction condition predicted by the RSM model was used to perform the extraction of AChE. Then the crude enzyme extract was subjected to AChE activity measurement. The experimentally validated AChE activity was used to compare with the model-predicted activity. And lastly the model validity was tested by evaluating the agreement between the predicted and experimental activity, as well as by considering the confidence intervals generated by the RSM analysis.

Enzyme Activity Assay

As described by Nazri et al. [7], AChE activity will be determined using a modified Ellman assay. 800 µL of 0.1 M sodium phosphate buffer at pH 7, 80 µL of 0.1 mM 5,5′-Dithiobis(2-nitrobenzoic acid) (DTNB), and 40 µL of crude enzyme extract were added to a cuvette. Then 20 µL of acetylthiocholine iodide (ATC) was added to the same cuvette and mixed evenly by using a pipette. The absorbance of the mixture was measured using a spectrophotometer at 412 nm. The absorbance was recorded and used to calculate the AChE activity using the equation as follows:

$$Enzyme\ Activity\ (U) = \frac{\Delta A/\min \times V_{total}}{\varepsilon \times l} \quad \text{(Eqn. 3)}$$

which ΔA/min is the change in absorbance per minute, V_{total} is the total volume of the reaction mixture, ε is the molar extinction coefficient of TNB, and l is the path length.

Protein Quantification Assay

Protein concentration was quantified using the Bradford protein assay, with bovine serum albumin (BSA) serving as the standard. 10 µL of diluted enzyme crude extract was added to the microplate, then 190 µL of diluted Bradford reagent was added to the well. The mixture was incubated for 10 minutes, then the absorbance was measured using a microplate reader at 595 nm.

Enzyme Kinetics

The kinetics of AChE was determined under optimized extraction conditions obtained from RSM. The enzyme kinetics was evaluated by measuring the AChE activity at different concentrations of three different synthetic substrates (ATC, PTC, BTC) with concentrations ranging from 0.1 mM to 2.0 mM. The enzyme activity was measured using Ellman's assay as mentioned above. Then the Michaelis-Menten curve was plotted using GraphPad Prism software version 10.6.1 to determine the maximal catalytic rate (V_{max}) and the biomolecular constant (K_m) [10].

RESULT AND DISCUSSION

Optimization of AChE Extraction Condition using OFAT

Optimization of NaCl concentration

The AChE extraction was performed at NaCl concentrations ranging from 0 to 0.30 M to optimize the salt concentration in the extraction buffer using OFAT. Based on **Fig. 1**, the AChE activity increases as the concentration of NaCl increases and reaches a maximum at 0.15 M and followed by a decrease of activity as the salt concentration increases. The statistical analysis using one-way ANOVA showed that the effect of NaCl concentration was not statistically significant on AChE activity, which gave a p-value of 0.3602 ($p > 0.05$).

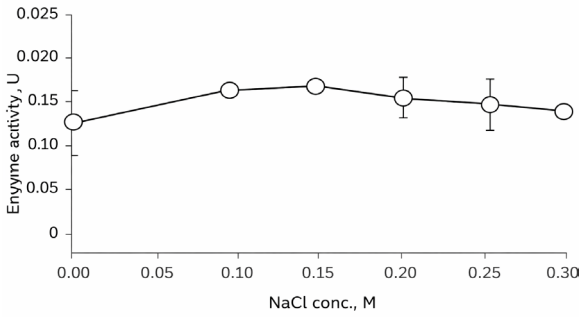

Fig. 1. Optimization of the NaCl concentration ranging from 0 M to 0.30 M in the extraction buffer for acetylcholine (AChE) extraction under OFAT approach.

The optimal concentration of NaCl for the extraction of AChE was observed at 0.15 M. This is because low NaCl concentration will improve the enzyme solubility and stabilize the electrostatic interactions of the protein. Kamal and Al-Jafari [11], state that NaCl weakens the electrostatic bonding of AChE with the membrane protein, which increases the solubility of the enzyme. However, high salt concentration leads to a decrease in the AChE activity. This result is aligned with the one reported by Smissaert [12], who mentions that the rate of acetylcholine hydrolysis at low substrate concentration decreases as the salt concentration increases, further indicating that higher NaCl concentrations are inhibitory.

Optimization of Triton X-100 concentration

The effect of Triton X-100 concentration on AChE extraction was tested using OFAT. The Triton X-100 concentration range from 0 to 0.10% was evaluated. According to **Fig. 2**, the AChE activity increased as the concentration of Triton X-100 increased and reached the maximum activity at 0.02% Triton X-100. After 0.02% Triton X-100, the AChE activity decreased. The statistical analysis showed that the effect of Triton X-100 concentration on AChE extraction was not statistically significant, obtaining a p-value of 0.1279 ($p > 0.05$) in one-way ANOVA.

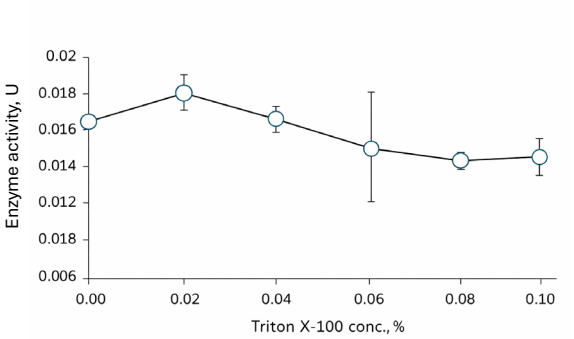

Fig. 2. Optimization of Triton X-100 concentration ranging from 0 to 0.10% Triton X-100 concentration for acetylcholinesterase (AChE) extraction using OFAT approach.

At low concentration, the activity of AChE increased. This is due to the low concentration of Triton X-100, which improves the solubilization of the membrane-bound AChE without affecting the enzyme structure and stability. The result is comparable with the one reported by Zimmermann et al. [13]. He reported a 115% increase in AChE activity by using a low concentration of Triton X-100 (0.01%). High concentration of Triton X-100 leads to increase in micelle formation, which will affect the substrate binding and result in low AChE activity [13].

Optimization of Buffer pH

The effect of buffer pH, ranging from pH 5.8 to 8.8 on AChE extraction was determined using OFAT, all the other extraction parameters were maintained at constant. Based on **Fig. 3**, the AChE activity was lowest at acidic pH (5.8 to 6.8) and increased as the pH increased. The highest AChE activity was obtained when the enzyme was extracted using an extraction buffer at pH 8.8 using Tris-HCl buffer, which indicates that the extraction of AChE is favored under slightly alkaline conditions. The effect of buffer pH on AChE activity was significant, which was confirmed by performing one-way ANOVA, obtaining a p-value of 1.83×10^{-5} ($p < 0.05$). This result proves that variations in pH influence the efficiency of the extraction significantly.

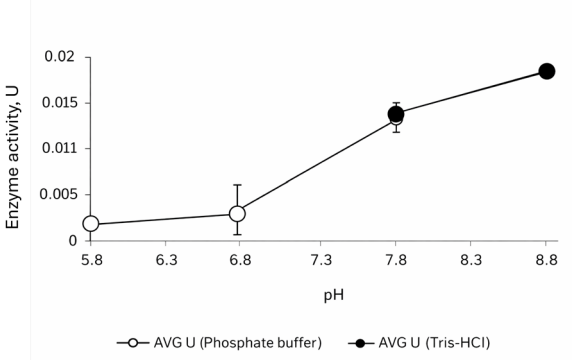

Fig. 3. Optimization of the extraction buffer pH for acetylcholinesterase (AChE) extraction using phosphate buffer (pH 5.8-7.8) and Tris-HCl buffer (pH 7.8-8.8) under OFAT approach.

The phosphate buffer was used for pH range from 5.8 to 7.8. This is because its pKa value is 7.2. According to Salz et al. [14] optimal buffering capacity occurs when the pH value is one unit above and below the pKa value. For slightly alkaline conditions (pH range from 7.8-8.8), Tris buffer is used because it has a pKa value of 8.3, and buffering capacity between pH 7 to 9. The extraction of AChE strongly depends on the pH of the extraction buffer. This is due to the ionization state of the amino acid residue, which contributes to the AChE structure and solubility. The histidine residue in the catalytic triad must be properly ionized to allow the catalytic activity of the enzyme [8]. At acidic pH, high proton concentration allows the protonation of the histidine imidazole group, which disrupts the substrate binding, therefore reducing the enzyme activity [15].

Optimization AChE Extraction Condition using RSM

Experimental Design and Model Development

The optimization of AChE extraction conditions was performed using response surface methodology (RSM) based on a three-factor Box Behnken Design (BBD). BBD was selected because it is an efficient second-order design. It enables the evaluation of linear, quadratic and interaction effects between parameters while requiring a small number of experimental runs compared to FFD and CCD [16]. Other than that, BBD allows the exploration of optimal conditions without testing extreme combinations of the factors [17]. This prevents the enzyme from being exposed to harsh conditions and compromises its stability and structure. Three independent variables, which are buffer pH, NaCl concentration, and Triton X-100 concentration, were chosen to be used in the RSM model. Among these parameters, pH has the strongest effect on AChE extraction. Even though NaCl concentration and Triton X-100 concentration were tested to not have a significant effect on the extraction efficiency ($p = 0.3602$ and $p = 0.1279$, respectively), they were retained in the RSM design to evaluate the interaction effect that cannot be tested by OFAT.

Statistical analysis of the RSM model

Analysis of variance (ANOVA) and Fisher's statistical test (F-test) were performed to evaluate the RSM model developed to optimize AChE extraction. The quadratic model generated using BBD was found to be statistically significant with a low model p-value of 0.0068 ($p < 0.05$) and F-value of 7.68 (**Table 3**). This confirmed that the AChE activity could be reliably explained by the selected independent variables [18]. Other than that, the lack-of-fit test of the model was not statistically significant ($p = 0.4974$). This indicates that the model adequately fits the experimental data, and the residual error is mainly due to random experimental variation.

Table 3. ANOVA analysis of the fitted Box-Behnken design (BBD).

Source	Sum of Squares	df	Mean Square	F-value	p-value
Model	0.0045	9	0.0005	7.68	0.0068
A-pH	0.0020	1	0.0020	31.60	0.0008
B-NaCl	0.0001	1	0.0001	1.66	0.2392
C-Triton X-100	0.0002	1	0.0002	2.56	0.1534
AB	0.0009	1	0.0009	13.44	0.0080
AC	9.805E-06	1	9805E-06	0.1517	0.7085
BC	0.0001	1	0.0001	1.81	0.2210
A^2	0.0012	1	0.0012	17.83	0.0039
B^2	0.0000	1	0.0000	0.2227	0.6513
C^2	8.727E-06	1	8.727E-06	0.1350	0.7242
Residual	0.0005	7	0.0001		
Lack-of-fit	0.0002	3	0.0001	0.9478	0.4974
Pure Error	0.0003	4	0.0001		
Cor Total	0.0049	16			

Note* df - degree of freedom.

Among the individual factors, pH of the buffer has the strongest influence on the AChE extraction with a highly significant linear effect ($p = 0.0008$) and quadratic effect ($p = 0.0039$). This suggests the presence of curvature in the response and indicates the presence of an optimal condition instead of a simple line trend Bezerra et al. [19]. In contrast, the effect of NaCl concentration and Triton X-100 concentration was not statistically significant. The individual effect of these parameters on AChE extraction was weaker. Statistically significant

interaction between pH and NaCl concentration (AB) was observed with a p-value of 0.0080, which suggests that the effect of ionic strength on AChE extraction is dependent on the pH of the extraction buffer. Other interactions (AC and BC) and the quadratic terms for NaCl and Triton X-100 were not significant.

The high coefficient of determination of the model (R^2 = 0.9081) further supports the good fit of the model (**Table 4**). This result indicates that approximately 90.8% of the variability in AChE activity could be explained by the quadratic regression model. The adjusted R^2 value of 0.7898 remained reasonably close to the R^2 value, which suggests that the included terms were relevant and that the model was not excessively over-parameterized. However, the predicted R^2 was low (predicted R^2 = 0.3048), model validation was conducted. The adequate precision value of 9.96, which exceeds the recommended threshold of 4, further confirms that the model possesses a sufficient signal-to-noise ratio and is suitable for navigating the experimental design space [20].

Table 4. Statistical summary of the fitted RSM model.

ANOVA	Value
R^2	0.9081
Adjusted R^2	0.7898
Predicted R^2	0.3048
Adeq Precision	9.9626

Note* Adeq Precision – Adequate Precision.

Effect of Independent Variables on AChE Activity

Table 5 summarizes the estimated regression coefficient of the studied factors (buffer pH, NaCl concentration, and Triton X-100 concentration) along with their confidence intervals and variance inflation factors (VIF). VIF is a diagnostic measure used to quantify how much the variance of a regression coefficient is inflated due to non-orthogonality or collinearity among predictors [21]. In an orthogonal design, the standard error of a coefficient estimate is at its minimum. However, in a design with collinearity, the standard error increases as the square root of the VIF increases. The VIF value of 1 indicates a perfect orthogonality, which means there is no correlation between the predictors. The VIF value above suggests potential collinearity issues. A VIF value exceeding 100 indicates severe multicollinearity, which leads to unreliable coefficient estimates. As shown in **Table 5**, all the predictors have VIF values close to 1, which indicates minor multicollinearity and stable coefficient estimates.

Table 5. Coefficients in terms of coded factors.

Factor	Coefficient Estimate	df	Standard Error	95% CI Low	95% CI High	VIF
Intercept	0.0880	1	0.0036	0.0795	0.0965	
A-pH	0.0160	1	0.0028	0.0093	0.0227	1.00
B-NaCl	0.0037	1	0.0028	-0.0031	0.0104	1.00
C-Triton X-100	0.0046	1	0.0028	-0.0022	0.0113	1.00
AB	0.0147	1	0.0040	0.0052	0.0242	1.00
AC	0.0016	1	0.0040	-0.0079	0.0111	1.00
BC	0.0054	1	0.0040	-0.0041	0.0149	1.00
A^2	0.0165	1	0.0039	0.0073	0.0258	1.01
B^2	-0.0018	1	0.0039	-0.0111	0.0074	1.01
C^2	-0.0014	1	0.0039	-0.107	0.0078	1.01

Note* df - degree of freedom. VIF - variance inflation factors. CI - confidence interval.

The confidence intervals provide further insights into the statistical significance of each coefficient. Positive coefficient estimates were observed for the majority of the factors. The main effect, pH, showed the highest positive coefficient (0.0160), followed by Triton X-100 (C, 0.0046) and NaCl (B, 0.0037). However, the confidence intervals for NaCl and Triton X-100 include zero. This suggests that these effects may not be statistically significant at the 95% confidence level [22]. The interaction effects between factors were also evaluated. It shows that the interaction between pH and NaCl was significant and positive (0.0147), while the other two-way interactions, which are pH and Triton X-100, and NaCl and Triton X-100, were not significant because their confidence intervals include zero. Quadratic effects reveal that pH^2 has a significant positive effect with a coefficient of 0.0165, reinforcing the strong influence of pH on the response. In contrast, $NaCl^2$ and Triton $X\text{-}100^2$ give a small negative coefficient (-0.0018 and -0.0014 respectively) and wide confidence intervals include zero, which indicates the quadratic effect is limited. The perturbation plot in **Fig. 4** visualizes the comparative effect of pH, NaCl concentration, and Triton X-100 on the AChE activity at a fixed point in the design space. The sensitivity of the AChE activity to the variation in each factor was indicated by the curves, when all the other factors are held constant at their central points.

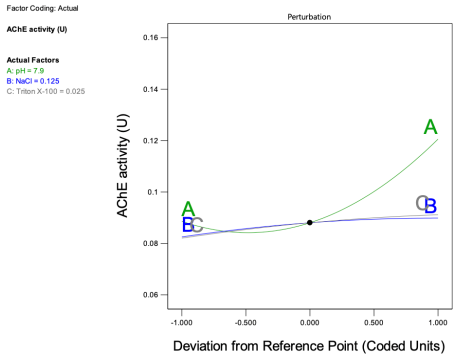

Fig. 4. Perturbation plot showing the effect of pH (A), NaCl concentration (B), and Triton X-100 concentration (C) on acetylcholinesterase (AChE) activity with other factors fixed at their center points.

According to the plot, pH has the steepest and upward-curving line. This suggests that it has the strongest influence on the AChE activity [23]. The positive slope suggests that increasing pH significantly increases the AChE activity. In contrast, NaCl and Triton X-100 show flatter curves, which indicates that their effect on the response is weaker and not significant, which is aligned with the regression coefficient analysis.

Buffer pH plays an important role in ionization states of the active-site residues, specifically the histidine residue in the catalytic triad [8]. Therefore, it has a strong influence on the AChE extraction. The ionization state of the histidine residue in the catalytic triad is highly sensitive to pH, it needs to be properly ionized to allow catalytic activity [24]. While NaCl and Triton X-100 mainly affect the solubility and the stability of the enzyme rather than catalytic activity.

Model Diagnostics

Model diagnostics were performed to evaluate the model adequacy, reliability, and statistical assumptions of the fitted quadratic response surface model for AChE extraction. This ensures that the model predictions are valid and statistically reliable. **Table 6** shows the agreement between experimental and model-predicted AChE activity together with the corresponding residuals and influence diagnostics. A close correspondence between experimental and predicted AChE activity was observed, which was reflected by a small residual value in every run. This indicates that the model accurately represents the

experimental data. No extreme residuals or unusually high leverage values were observed. This suggests that none of the experimental runs exerted excessive influence on the regression model [25].

Table 6. Experimental and the model-predicted acetylcholinesterase (AChE) activity, along with the residuals, and diagnostic statistics used for validation of the fitted response surface model.

RO	Actual Value	Predicted Value	Residual	Leverage	ISR
1	0.0922	0.0902	0.0021	0.750	0.519
2	0.0920	0.0880	0.0040	0.200	0.555
3	0.0756	0.0880	-0.0125	0.200	-1.732
4	0.0738	0.0785	-0.0046	0.750	-1.147
5	0.0848	0.0819	0.0028	0.750	0.698
6	0.0849	0.0802	0.0046	0.750	1.147
7	0.0956	0.0984	-0.0028	0.750	-0.698
8	0.0841	0.0880	-0.0040	0.200	-0.550
9	0.0764	0.0757	0.0007	0.750	0.179
10	0.0996	0.1003	-0.0007	0.750	-0.179
11	0.1109	0.1130	-0.0021	0.750	-0.519
12	0.0881	0.0842	0.0039	0.750	0.968
13	0.0936	0.0880	0.0056	0.200	0.777
14	0.1214	0.1252	-0.0039	0.750	-0.968
15	0.1438	0.1371	0.0067	0.750	1.666
16	0.0949	0.0880	0.0068	0.200	0.950
17	0.0911	0.0978	-0.0067	0.750	-1.666

Note* RO - Run Order. ISR - Internally Studentized Residuals. ESR – Externally Studentized Residuals. Cook's D - Cook's Distance. DFFITS - Difference in fits. SO - Standard Order.

The normal probability plot of externally studentized residuals was generated to validate the normality assumption of the residuals. Based on **Fig. 5**, the majority of the residuals were closely distributed along the line. This indicates that the residuals are approximately normally distributed and suggests that the deviations between experimental and predicted AChE activity are random and not systematically biased [20]. The approximate normality of residuals validates one of the key assumptions underlying analysis of variance (ANOVA) and regression analysis.

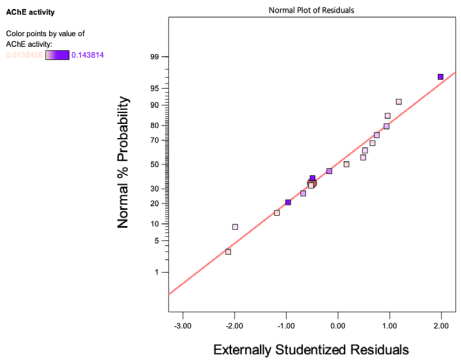

Fig. 5. Normal probability plot of the externally studentized residual for the fitted response surface model of acetylcholinesterase (AChE) activity.

The Box-Cox plot in **Fig. 6** was used to determine if a power transformation of the response variable was necessary to improve the model adequacy. The minimum Box-Cox curve was observed at a (λ) value close to 1. The 95% confidence interval for λ includes 1, therefore, no transformation of the AChE activity data was needed [26].

This indicates that the fitted quadratic model appropriately captures the relationship between the extraction parameters and AChE activity.

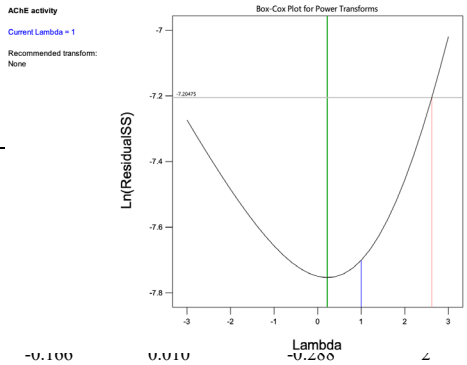

Fig. 6. Box-Cox plot for the Box-Behnken optimization studies.

The predicted versus the experimental AChE activity was plotted to evaluate the accuracy and the predictive capability of the response surface model. Based on **Fig. 7**, the experimental data points were clustered along the 45° line, which indicates a good agreement between the predicted and the experimental observed value. The analysis suggested that the quadratic model accurately describes the relationship between the extraction parameter and AChE activity, which indicates a reliable RSM model Bezerra et al. [19]. This observation is further supported by the high R^2 (0.9081) obtained from the ANOVA analysis (**Table 4**).

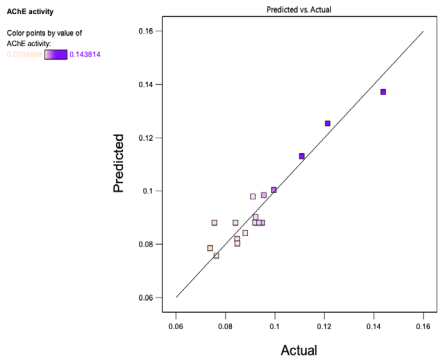

Fig. 7. Model-predicted versus experimental acetylcholinesterase (AChE) activity for the Box-Behnken studies.

To identify the experimental run that exerted a disproportionately large influence on the fitted model, the leverage versus run plot was generated. The leverage measures the deviation of an observation's predictor value from the center of the experimental design space, which high leverage points have potential to affect the model estimate strongly. Based on **Fig. 8**, all leverage values fall within the acceptable range from 0 to 1. This indicates that no experimental runs are excessively influential [25]. No single design point had an undue impact on the regression model, and that the model is robust and balanced.

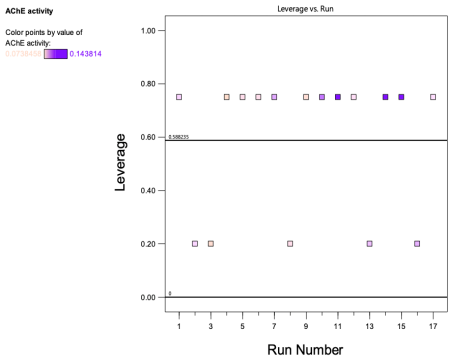

Fig. 8. Leverage values plotted against run number for the Box-Behnken studies.

Next, Cook's distance was calculated to evaluate the influence of each experimental run on the fitted model. It combines residual magnitude and leverage to provide a comprehensive measure of how much an individual observation affects the estimated regression coefficients. All the experimental runs have Cook's distance below the threshold value 1 (**Fig. 9**). This indicates that not a single observation gives excessive influence on the model, which confirms that the regression coefficient and the predicted AChE activity are not disproportionately driven by any individual run [27]. This result is consistent with the leverage and residual diagnostics.

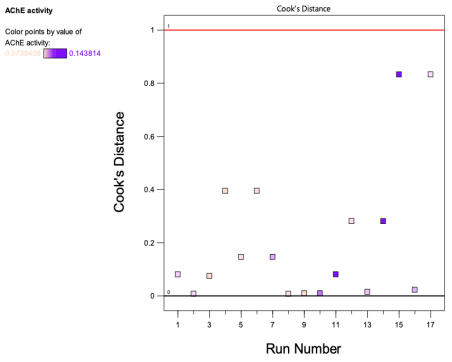

Fig. 9. Cook's distance versus the run number plot for the Box-Behnken studies.

The externally studentized residuals were plotted against the experimental run order to identify any systematic trends or time-related effects associated with the order of the experimentation [28]. As shown in **Fig. 10**, the residuals are randomly distributed above and below the zero line without exhibiting systematic trends. This observation suggests that the experimental errors are independent and are not influenced by the sequence of experimentation. It confirmed that no bias or hidden factors were introduced during the sequential execution of the experiment. All the external studentized residuals were observed within the acceptable range (±4.82), indicating that no experimental run has unusually large deviations from the model prediction, which confirms the absence of outliers and supports the stability and reproducibility of the experimental procedure.

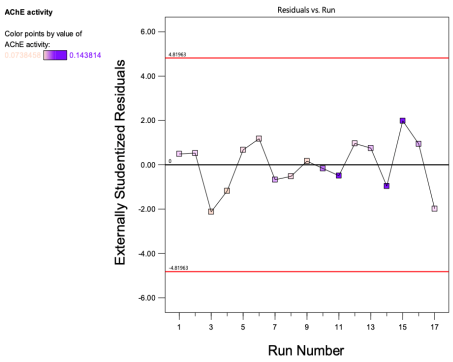

Fig. 10. The residuals versus the run number plot for Box-Behnken studies.

Difference in Betas (DFBETAS) and Difference in Fits (DFFITS) diagnostics were done to assess the effect of individual experimental runs on the response surface model for AChE activity. DFBETAS quantifies how much a specific regression coefficient changes when an individual observation is removed from the model, while DFFITS evaluates the impact of a single observation on its own predicted values [29]. Most of the DFBETAS and DFFITS values are observed within the threshold limits (±0.73 and ±2.30, respectively) (**Fig. 11** and **Fig. 12**).

This indicates that most of the observations did not exert excessive influence on the model [30]. However, run 3 exceeded the DFBETAS threshold for the interception (**Fig. 11**), while run 15 and 17 exceeded the DFFITS threshold (**Fig. 12**). This suggests that these runs exert a stronger influence on the regression coefficient. Although influential, they do not dominate the model excessively, because their leverage, residual, and Cook's distance values are acceptable. This behavior is expected in BBD. This is because the factorial points are located farther from the center of the experimental domain, which contributes more information to the estimation of model parameters.

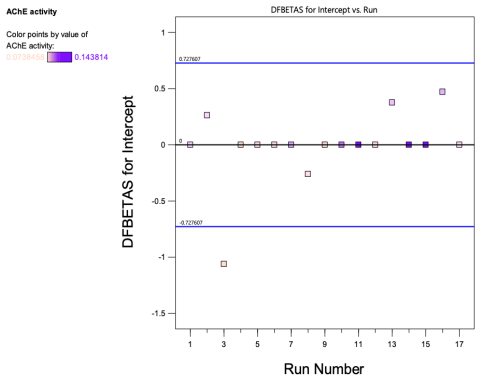

Fig. 11. Difference in Betas (DFBETAS) plot for the intercept plotted against run order for the Box-Behnken studies.

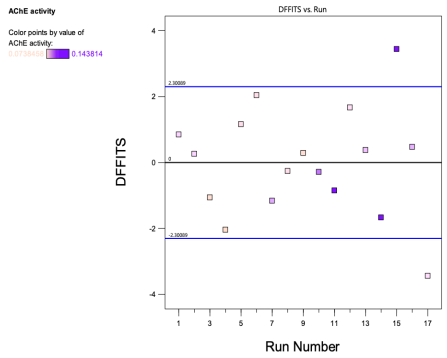

Fig. 12. Difference is Fits (DFFITS) value plotted against the run order for the Box-Behnken studies.

Response Surface Analysis

The 3D response surface curves were generated using the regression model developed in Design-Expert. These 3D plots visualize the interactive effects of the studied factors (pH, NaCl concentration, Triton X-100 concentration) on AChE activity, while the third factor was maintained at the center level. This capability of the response surface approach makes it better compared to OFAT.

Interaction between NaCl concentration and Triton X-100 concentration

When pH was maintained at its midpoint value of 7.9, the effects of NaCl concentration and Triton X-100 concentration on enzyme activity were explored. With the pH fixed at its center level (pH 7.9), numerical optimization was carried out with NaCl and Triton X-100 under experimental ranges. This workflow is meant to identify the predicted response under these constraints. A point prediction was subsequently generated using the fitted quadratic model and produced an AChE activity of 0.098 U with a 95 percent confidence interval ranging from 0.082 to 0.115 U. This was achieved at a NaCl and Triton X-100 concentrations of 0.2 M and 0.04%, respectively (**Fig. 13**). Compared with other conditions, this predicted activity is lowest (0.098 units), suggesting that increasing NaCl to 0.20 M and Triton X-100 to 0.04% (v/v) provided a lower enhancement of enzyme performance.

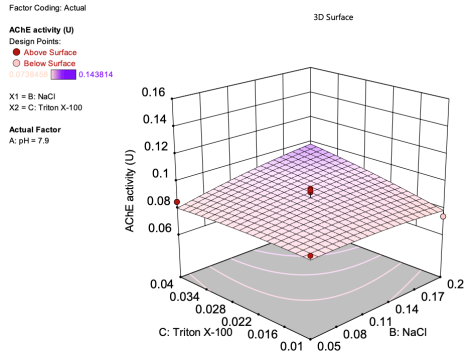

Fig. 13. The 3D response surface curve that shows the interaction between Triton X-100 concentration and NaCl concentration with pH fixed at the center level.

The 3D response surface plot (**Fig. 13**) revealed a relatively flat plane with no noticeable curvature, indicating that within the tested ranges, both NaCl and Triton X-100 had negligible effects on enzyme activity [31].

The absence of significant interaction or curvature suggests that enzyme activity remained stable regardless of changes in NaCl or Triton X-100 concentrations. This indicates that ionic strength and surfactant levels do not play a critical role in modulating enzyme performance under the studied conditions. Instead, enzyme activity is likely governed more strongly by other parameters, such as pH, which showed dominant effects in previous analyses. Overall, the response surface indicates that NaCl and Triton X-100 concentrations exert minimal influence on enzyme activity, supporting the conclusion that optimization efforts should focus primarily on pH rather than on these two variables.

Interaction between pH and Triton X-100 concentration

The interaction between pH and Triton X-100 concentrations was tested with the NaCl concentration fixed at the center level (0.125 M). Based on **Fig. 14**, the model predicted a maximum AChE activity of 0.125 units (95% CI: 0.109 to 0.142) based on numerical optimization followed by point prediction as before, which was achieved at a pH and Triton X-100 concentrations of 8.8 and 0.04%, respectively. This activity level is higher than that observed when pH was fixed at 7.9 (0.098 units), confirming that increasing pH to 8.8 and Triton X-100 to 0.04% (v/v) synergistically enhances enzyme activity.

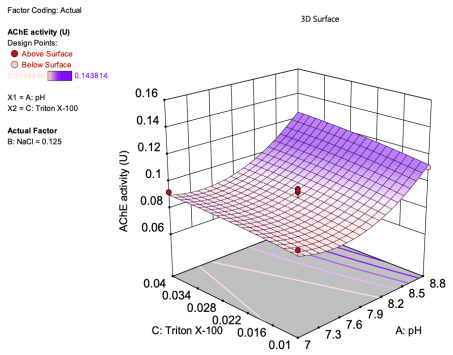

Fig. 14. The 3D response surface curve that shows the interaction between Triton X-100 concentration and pH with NaCl concentration fixed at the center level.

The 3D surface plot (**Fig. 14**) demonstrates a clear upward curvature along the pH axis, confirming that pH is the primary factor influencing the response. In contrast, variation in Triton X-100 concentration produced only a minor effect, as indicated by the relatively flat slope along the C-axis. These findings emphasize the importance of alkaline pH as the primary driver of enhanced enzyme performance [8], with Triton X-100 providing a lesser but supportive effect under optimized conditions. Although NaCl at its midpoint level does not independently maximize activity, maintaining it at 0.125 M ensures system stability while allowing pH and Triton to exert their stronger influence.

Interaction between pH and NaCl concentration

When the concentration of Triton X-100 was held constant at its midpoint value of 0.0250% (v/v), the effects of pH and NaCl concentration on enzyme activity were investigated. The response surface analysis revealed that the maximum enzyme activity of 0.137 units (95% CI: 0.121 to 0.154) is based on numerical optimization followed by point prediction as before. This was achieved at a pH of 8.8 and a NaCl concentration of 0.20 M (**Fig. 15**).

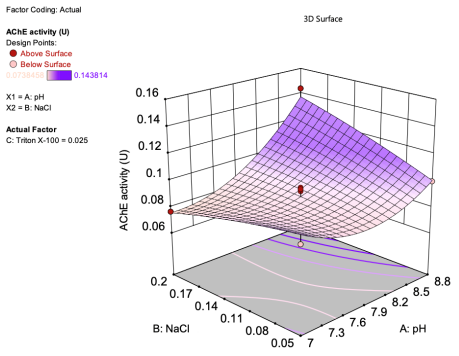

Fig. 15. The 3D response surface curve that shows the interaction between pH and NaCl concentration with Triton X-100 concentration fixed at the center level.

When the Triton X-100 concentration was fixed at its midpoint (0.025% v/v), the 3D surface plot (**Fig. 15**) demonstrated a pronounced curvature, highlighting a strong interaction between pH and NaCl concentration. The surface slopes upward with increasing pH, confirming pH as the dominant factor influencing the response. In contrast, changes in NaCl concentration produced only marginal effects, consistent with its weaker perturbation slope. The plot further illustrates that the maximum predicted enzyme activity occurs at higher pH values, regardless of NaCl concentration, suggesting that the availability of ionized imidazole groups at elevated pH levels facilitates catalysis of the substrate [8,15]. In short, the optimal conditions suggest that alkaline pH enhances the ionization of active sites, thereby favoring substrate binding and catalytic turnover. In parallel, the elevated NaCl concentration may have contributed to structural stabilization of the enzyme by modulating ionic strength, without imposing inhibitory effects within the tested range [11].

Collectively, buffer pH is the primary determinant of AChE activity, while NaCl and Triton X-100 serve as supporting factors. This observation was aligned with the OFAT result and also the diagnostic analysis. The observed curvature in the response surface plot further supports the suitability of a quadratic model in optimization and indicates the existence of an optimal region rather than a linear trend.

Predicted Optimized Extraction Condition and Model Validation

Numerical optimization was performed to maximize the AChE activity under the examined parameter range. The optimum extraction condition was predicted by the model, which at a pH of 8.79, NaCl concentration of 0.197 M, and Triton X-100 concentration of 0.039% (v/v) yielded a maximum AChE activity of 0.145 units (95% CI: 0.125 to 0.166) (**Table 7**). The alkaline pH gave the most significant influence on AChE activity, which was consistent with the earlier findings using OFAT. The relatively narrow confidence interval indicates the model has a strong reliability [32].

Table 7. The model predicted optimum extraction conditions and maximum AChE activity based on the Box-Behnken design.

Factor	Optimized Condition	Low Level	High Level	Predicted AChE activity, U (95%, C.I.)
pH	8.79	7.00	8.80	0.145
NaCl (M)	0.1967	0.05	0.20	(0.125 to 0.166)
Triton X-100 (% (v/v))	0.0393	0.01	0.04	

Note* CI - confidence interval.

Model validation was done to evaluate the model's predictive capability by conducting the extraction of AChE under predicted optimum conditions. As shown in **Table 8**, it yields a maximum AChE activity of 0.152 units (95% CI: 0.145 to 0.159), which shows an overlapped 95% confidence interval between the predicted activity and the actual activity. This suggests that there was no significant difference between the predicted result and the experimentally validated result at the 95% confidence level. Further confirmed that the model was statistically reliable.

Table 8. Verification results between the experiments and the predicted response.

Factor	Optimized Condition	RSM Prediction (95%, C.I.)	Experimental Validation (95%, C.I.)
pH	8.79	0.145	0.152
NaCl	0.1967 M	(0.125 to 0.166)	(0.145 to 0.159)
Triton X-100	0.0393 %		

Note* C.I. - confidence interval.

Comparison between OFAT and RSM

Table 9 summarizes the comparison between OFAT and RSM approach based on the optimum extraction condition and the AChE activity. By using the OFAT approach, the optimum extraction conditions were determined by changing individual factors independently, while keeping the other factors at constant. This method successfully identifies the general trends for pH, NaCl concentration, and Triton X-100 concentration. However, it ignored the interaction between these parameters. In contrast, RSM simultaneously evaluated the combined effects of multiple variables and their interactions through a statistically designed experimental matrix.

The comparison between OFAT approach and RSM approach in optimization of extraction condition also revealed that the optimum condition obtained through OFAT and RSM was different, which OFAT suggest that the optimum extraction condition is at pH of 8.8, NaCl concentration of 0.15 M and Triton X-100 concentration of 0.02% (v/v), while the RSM model suggest that the optimum extraction condition is at pH of 8.8, 0.1967 M NaCl concentration and 0.0393% (v/v) Triton X-100 concentration. This difference is due to RSM being able to capture the interaction between factors, while OFAT cannot, therefore giving a different result [19]. The optimum extraction condition obtained from the RSM approach yields a higher AChE activity of 0.152 units (95% CI: 0.145 to 0.159) compared to OFAT (**Table 9**). This suggests that the interaction between parameters captured by RSM has effects on the AChE activity. This made the RSM approach one step above the OFAT approach. This advantage of RSM has been reported by Bezerra et al. [19] and Helmiyati et al. [33] in their research.

Table 9. The comparison between the optimum extraction conditions and AChE activity obtained between OFAT and RSM.

	OFAT		RSM	
Factor	Optimum Value	Activity, U (95% C.I.)	Optimum Value	Activity, U (95% C.I.)
pH	8.8	0.125 (0.118 - 0.132)	8.79	0.152 (0.145 to 0.159)
NaCl	0.15 M		0.1967 M	
Triton X-100	0.02 % (v/v)		0.0393 % (v/v)	

Note* C.I. - confidence interval.

Enzyme Kinetics

The Michaelis-Menten model was used to evaluate the kinetics of the AChE under different substrate concentrations using acetylthiocholine iodide (ATC), propionylthiocholine iodide (PTC), and butyrylthiocholine iodide (BTC) as substrates. Based on **Fig. 16**, the rate of reaction increases rapidly at low

concentrations of substrates and reaches a plateau at high substrate concentrations. ATC exhibited the highest maximum reaction velocity (V_{max} = 0.0224 U), followed by PTC (V_{max} = 0.0214 U) and BTC (V_{max} = 0.0193 U). Moreover, Michaelis constant (K_m) reflects the affinity of AChE for each substrate. ATC has the lowest K_m value (0.0339 mM) compared to PTC (0.2177 mM) and BTC (0.2316 mM).

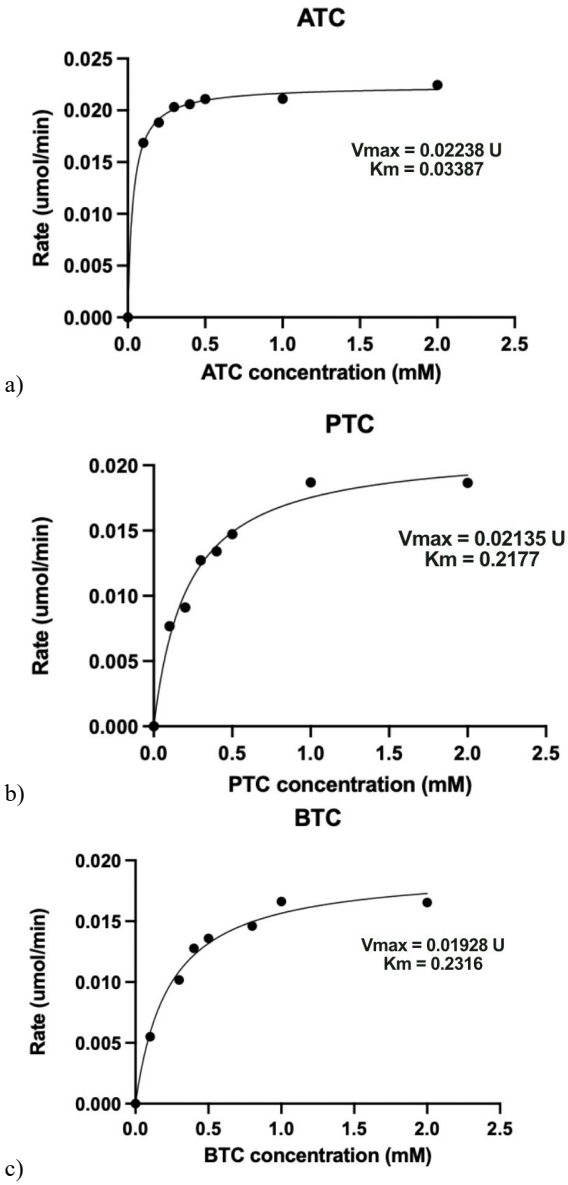

Fig. 16. Michaelis–Menten plots of acetylcholinesterase (AChE) activity using different substrates: (a) acetylthiocholine (ATC), (b) propionylthiocholine (PTC), and (c) butyrylthiocholine (BTC). Initial reaction rates were measured at increasing substrate concentrations and fitted to the Michaelis–Menten equation to determine the kinetic parameters V_{max} and K_m for each substrate.

The result shows that ATC has the highest V_{max} (0.0224 U) and lowest K_m (0.0339 mM), which indicates that the AChE catalyzes the hydrolysis of ATC fastest and ATC has the strongest affinity to the AChE. This observation is consistent with the one reported by Khalidi et al. [10], which states that AChE affinity to ATC was higher compared to BTC and PTC. AChE hydrolyses ATC most efficiently, followed by PTC and BTC [34]. By studying enzyme kinetics, it was confirmed that the enzyme extracted from the brain of *S.commerson* was AChE and not other cholinesterases. As a summary, it is known that the extraction efficiency and catalytic activity of acetylcholinesterase (AChE) are significantly influenced by the biochemical microenvironment, which includes pH and ionic strength. These factors directly affect protein folding, charge stabilization, and enzyme–substrate interactions. The catalytic triad of serine, histidine, and glutamate/aspartate residues in AChE needs to have the right balance of electrostatic forces, which is strongly influenced by the pH. For instance, the imidazole group of histidine is optimum when the pH is somewhat alkaline (around 8–9). This allows the histidine residue inside the catalytic triad to function as a universal base, which enables the nucleophilic assault of the serine hydroxyl on the substrate's acetyl group. Dvir et al. [35] assert that suboptimum environmental pH leads to a charge of the ionizable group. For instance, acidic conditions lead to histidine being protonated. Under this condition, nucleophilic activation will be harder, while too alkaline a condition can lead to structural residues losing their protons. All these lead to a local unfolding or destabilization of the structure.

The electrostatic stabilization of the active sites is also influenced by pH. The electrostatic potential surrounding the catalytic gorge in the active sites, which is a deep, narrow cavity, is determined by the surface charge distribution of AChE [35]. Any disruption of pH will change this landscape and affect substrate binding and conversion to product. Thanks to proper folding and charge complementarity, the substrate's choline moiety lines up perfectly with the anionic subsite. The anionic subsite is stabilized through π–cation interactions with the aromatic residues tryptophan and tyrosine [36]. Preservation of the pH close to the enzyme's isoelectric zone will help keep the secondary and tertiary structures intact and prevent denaturation or aggregation of the enzyme.

The ionic strength, which is controlled by the amount of NaCl, is very important for protein solvation and conformational dynamics. A low to moderate range of ionic strength (0.1–0.2 M NaCl) protects surface charges, and this can improve protein solubility. This lowers intermolecular repulsion and keeps enzymes soluble [37]. However, a high ionic strength can cause hydrophobic collapse through the breakup of the intramolecular salt bridges. This makes the molecule less flexible and less effective in catalyzing reactions, and in our study, this occurs at concentrations exceeding 0.2 M NaCl.

CONCLUSION

This study successfully optimized the extraction of acetylcholinesterase (AChE) from the brain tissue of *Scomberomorus commerson* using Response Surface Methodology (RSM). A Box–Behnken Design (BBD) was employed to systematically evaluate the effects of buffer pH, NaCl concentration, and Triton X-100 concentration on AChE extraction. The developed quadratic model demonstrated a good fit to the experimental data, as reflected by a high coefficient of determination (R^2 = 0.9081), a non-significant lack-of-fit, and an adequate precision value exceeding the recommended threshold, indicating strong model reliability and predictive capability. Among the investigated parameters, buffer pH was identified as the most influential factor governing AChE extraction efficiency. Both linear and quadratic effects of pH were statistically significant, highlighting the presence of an optimal alkaline extraction environment. Numerical optimization predicted optimal extraction conditions at pH 8.79, 0.197 M NaCl, and 0.039% Triton X-100, yielding a predicted AChE activity of 0.145 U (95% CI: 0.125 to 0.166). Experimental validation under these conditions produced a comparable activity of 0.152 U (95%

CI: 0.145 to 0.159), confirming the accuracy and robustness of the RSM model. In addition, enzyme kinetic characterization under optimized extraction conditions revealed substrate-dependent catalytic behavior. ATC exhibited the lowest K_m and highest V_{max}, indicating the highest substrate affinity and catalytic efficiency. Overall, this study establishes a reliable and reproducible extraction protocol for AChE from *S. commerson* brain tissue and demonstrates the superiority of RSM over OFAT in capturing complex variable interactions. Although this study achieved its objectives, several recommendations are proposed to further enhance and expand the scope of future research. Future studies may incorporate additional factors such as extraction temperature, buffer ionic strength, homogenization time, or protease inhibitors into the RSM design to further improve enzyme yield and stability. Other than that, the optimized crude extract may be subjected to partial or full purification techniques, such as ammonium sulfate fractionation, ion-exchange chromatography, or affinity chromatography, to evaluate purity, specific activity, and long-term enzyme stability. Last but not least, the extracted AChE can be used in inhibitor screening assays using organophosphate and carbamate compounds to assess its suitability as a biosensing element for environmental and food safety monitoring.

REFERENCES

1. Cao J, Li B, Li X. Identification of alzheimer's disease brain networks based on EEG phase synchronization. Biomed. Eng. OnLine 2025;24:32. https://doi.org/10.1186/s12938-025-01361-0
2. Ong SC, Tay LX, Ong HM, Tiong IK, Ch'ng ASH, Parumasivam T. Annual societal cost of alzheimer's disease in Malaysia: a micro-costing approach. BMC Geriatr. 2025;25:154. https://doi.org/10.1186/s12877-025-05717-y
3. Tang J, Feng J, Liang H, Pang Y, Tang Z, Chen Z, et al. Rapid and simple sensing of acetylcholinesterase and inhibition activity by utilizing a portable raman spectrometer. Talanta 2025;293:128086. https://doi.org/10.1016/j.talanta.2025.128086
4. Shi L, Yang F, Xu Y, Wang S. Expression of drosophila melanogaster acetylcholinesterase (DmAChE) gene splice variants in pichia pastoris and evaluation of its sensitivity to organophosphorus pesticides. J. Zhejiang Univ.-Sci. B 2021;22:204–13. https://doi.org/10.1631/jzus.B2000525
5. Kamaruzaman NA, Leong Y-H, Jaafar MH, Mohamed Khan HR, Abdul Rani NA, Razali MF, et al. Epidemiology and risk factors of pesticide poisoning in malaysia: a retrospective analysis by the national poison centre (NPC) from 2006 to 2015. BMJ Open 2020;10:e036048. https://doi.org/10.1136/bmjopen-2019-036048
6. Asaad SM, Inayat A, Ghenai C, Shanableh A. Response surface methodology in biodiesel production and engine performance assessment. Int. J. Thermofluids 2024;21:100551. https://doi.org/10.1016/j.ijft.2023.100551
7. Nazri MAFS, Basirun AA, Manogaran M, Khalidi SAM, Sabullah MK, Shukor MY. Optimisation of acetylcholinesterase extraction from the brain of clarias batrachus using response surface methodology. Bioremediation Sci. Technol. Res. 2019;7:5–8. https://doi.org/10.54987/bstr.v7i2.485
8. Assis CRD, Linhares AG, Oliveira VM, França RCP, Carvalho EVMM, Bezerra RS, et al. Comparative effect of pesticides on brain acetylcholinesterase in tropical fish. Sci. Total Environ. 2012;441:141–50. https://doi.org/10.1016/j.scitotenv.2012.09.058
9. Mororó MCC, Mahnke LC, Assis CRD, Da Silva RA, Cabrera MP, Bezerra RP, et al. Acetylcholinesterase purification from human erythrocytes using magnetic nanoparticles containing procainamide. Int. J. Biol. Macromol. 2024;269:132094. https://doi.org/10.1016/j.ijbiomac.2024.132094
10. Khalidi SAM, Sabullah MK, Sani SA, Ahmad SA, Shukor MY, Jaafar' I N M, et al. Acetylcholinesterase from the brain of Monopterus albus as detection of metal ions. J. Phys. Conf. Ser. 2019;1358:012028. https://doi.org/10.1088/1742-6596/1358/1/012028
11. Kamal MA, Al-Jafari AA. The preparation and kinetic analysis of multiple forms of human erythrocyte acetylcholinesterase. Prep. Biochem. Biotechnol. 1996;26:105–19. https://doi.org/10.1080/10826069608000057
12. Smissaert HR. Acetylcholinesterase: evidence that sodium ion binding at the anionic site causes inhibition of the second-order hydrolysis of acetylcholine and a decrease of its p K α as well as of deacetylation. Biochem. J. 1981;197:163–70. https://doi.org/10.1042/bj1970163
13. Zimmermann M, Westwell MS, Greenfield SA. Impact of detergents on the activity of acetylcholinesterase and on the effectiveness of its inhibitors. bchm 2009;390:19–26. https://doi.org/10.1515/BC.2009.005
14. Salz U, Mücke A, Zimmermann J, Tay FR, Pashley DH. pKa value and buffering capacity of acidic monomers commonly used in self-etching primers. J. Adhes. Dent. 2006;8:143–50
15. Marinho CS, Matias MVF, Brandão IGF, Santos EL, Machado SS, Zanta CLPS. Characterization and kinetic study of the brain and muscle acetylcholinesterase from danio rerio. Comp. Biochem. Physiol. Part C Toxicol. Pharmacol. 2019;222:11–8. https://doi.org/10.1016/j.cbpc.2019.04.005
16. Narukulla S, Bogadi S, Tallapaneni V, Sanapalli BKR, Sanju S, Khan AA, et al. Comparative study between the full factorial, box–behnken, and central composite designs in the optimization of metronidazole immediate release tablet. Microchem. J. 2024;207:111875. https://doi.org/10.1016/j.microc.2024.111875
17. Ferreira SLC, Bruns RE, Da Silva EGP, Dos Santos WNL, Quintella CM, David JM, et al. Statistical designs and response surface techniques for the optimization of chromatographic systems. J. Chromatogr. A 2007;1158:2–14. https://doi.org/10.1016/j.chroma.2007.03.051
18. Sibanda W, Pretorius P. Comparative study of the application of box behnken design (BBD) and binary logistic regression (BLR) to study the effect of demographic characteristics on HIV risk in south africa. 2012;1:15–40
19. Bezerra MA, Santelli RE, Oliveira EP, Villar LS, Escaleira LA. Response surface methodology (RSM) as a tool for optimization in analytical chemistry. Talanta 2008;76:965–77. https://doi.org/10.1016/j.talanta.2008.05.019
20. Dean A, Voss D, Draguljić D. Design and analysis of experiments 2017. https://doi.org/10.1007/978-3-319-52250-0
21. Sarabia LA, Ortiz MC. Response surface methodology. Compr. Chemom. 2009:345–90. https://doi.org/10.1016/B978-044452701-1.00083-1
22. Sedgwick P. Confidence intervals, P values, and statistical significance. BMJ 2015;350:h1113–h1113. https://doi.org/10.1136/bmj.h1113
23. Sivamaran V, Kavimani V, Bakkiyaraj M, Selvamani ST. Multi response optimization on tribo-mechanical properties of CNTs/nSiC reinforced hybrid al MMC through RSM approach. Forces Mech. 2022;6:100069. https://doi.org/10.1016/j.finmec.2021.100069
24. Hayat NM, Ahmad SA, Shamaan NA, Sabullah MK, Shukor MYA, Syed MA, et al. Characterisation of cholinesterase from kidney tissue of asian seabass (lates calcarifer) and its inhibition in presence of metal ions. J. Environ. Biol. 2017;38:383–8. https://doi.org/10.22438/jeb/38/3/MRN-987
25. Chatterjee S, Hadi AS. Influential observations, high leverage points, and outliers in linear regression. Stat. Sci. 1986;1:379–93
26. Qin J, Wang J, Follmann D. Bootstrap box–cox transformation likelihood ratio confidence intervals for the median in small sample problems. Stat. Biosci. 2025. https://doi.org/10.1007/s12561-025-09498-1
27. Cook RD. Cook's Distance. Int. Encycl. Stat. Sci. 2011:301–2. https://doi.org/10.1007/978-3-642-04898-2_189
28. Vining G. Technical advice: residual plots to check assumptions. Qual. Eng. 2010;23:105–10. https://doi.org/10.1080/08982112.2011.535696
29. Camilleri C, Alter U, Cribbie RA. Identifying influential observations in multiple regression. Quant. Methods Psychol. 2024;20:96–105. https://doi.org/10.20982/tqmp.20.2.p096
30. Suboh S, Aziz IA. Discovering patterns and deviations in data: comparison of anomaly detection procedure in regression. Adv. Appl. Stat. 2024;91:1195–215. https://doi.org/10.17654/0972361724063
31. Ockuly RA, Weese ML, Smucker BJ, Edwards DJ, Chang L. Response surface experiments: a meta-analysis. Chemom. Intell.

Lab. Syst. 2017;164:64–75. https://doi.org/10.1016/j.chemolab.2017.03.009
32. Terry L, Kelley K. Sample size planning for composite reliability coefficients: accuracy in parameter estimation via narrow confidence intervals. Br. J. Math. Stat. Psychol. 2012;65:371–401. https://doi.org/10.1111/j.2044-8317.2011.02030.x
33. Helmiyati H, Hapsari JV, Bakri R, Abdullah I, Umar A, Bagus Apriandanu DO. Nanocellulose-coated magnetite–strontium oxide as novel green catalyst for biodiesel production from waste cooking oil: optimization using RSM. Fuel 2025;396:135236. https://doi.org/10.1016/j.fuel.2025.135236
34. Guedes RNC, Zhu KY, Kambhampati S, Dover BA. Characterization of acetylcholinesterase purified from the lesser grain borer, rhyzopertha dominica (coleoptera: bostrichidae). Comp. Biochem. Physiol. C Pharmacol. Toxicol. Endocrinol. 1998;119:205–10. https://doi.org/10.1016/S0742-8413(97)00208-9
35. Dvir H, Silman I, Harel M, Rosenberry TL, Sussman JL. Acetylcholinesterase: From 3D structure to function. Chem Biol Interact. 2010;187(1–3):10–22. https://doi.org/10.1016/j.cbi.2010.01.042
36. Guengerich FP. Mechanisms of enzyme catalysis and inhibition. In: Comprehensive Toxicology. Elsevier; 2026. p. 58–66.
37. Kermasha S, Eskin MNA. Enzymes. In: Enzymes. Elsevier; 2021. p. 15–44.